

Direct string magnetic gradiometer for space applications

Andrew Sunderland^{a,*}, Alexey V Veryaskin^{a,b},
Wayne McRae^{a,b}, Li Ju^a, David G Blair^a

^a*School of Physics, University of Western Australia, Perth, WA, Australia*

^b*Gravitec Instruments, Perth, WA, Australia*

Abstract

Recently, a novel Direct String Magnetic Gradiometer (DSMG) has been developed, where a vibrating wire, driven by an AC current, is used as a single sensitive element. It is designed to directly measure the local off-diagonal components of the magnetic gradient tensor, B_{xz} , B_{yz} and B_{xy} , provided the distance to an object creating magnetic anomalies is much larger than the length of the string. This requirement is well satisfied in space, if the sensor is deployed from a satellite platform orbiting near the planet under surveillance. Current instruments operating at 1 kPa pressure achieve sensitivity of 1.8×10^{-10} T/m in the band 0.0001 Hz to 0.1 Hz. In this paper we show that proposed modifications to the current gradiometer design, specifically aimed at the deployment in space, could have a magnetic gradient sensitivity better than 10^{-13} T/m/ $\sqrt{\text{Hz}}$ in the frequency range of interest for specific missions both for fundamental research and for such applications as geophysical exploration on Mars and other solar system planets. Also, by combining a few single-axis magnetic gradiometer modules, it is possible to deploy a full tensor magnetic gradiometer.

Key words: magnetic gradients, gradiometry, magnetometry, current carrying string

1 Introduction

Magnetic gradiometry, as a powerful tool for magnetic anomaly mapping, have been discussed in literature in conjunction with future planetary and

* Corresponding author. Tel.: +61 422 282 438.

Email address: asund@physics.uwa.edu.au (Andrew Sunderland).

deep space missions (see for example Alves and Madeira[1][2]). Although conventional magnetometers are more commonly deployed on satellites, interest is growing in the use of magnetic gradiometers to extract data that cannot be obtained from magnetic field measurements alone. Hastings et al[3] described several advantages of using a magnetic gradiometer to directly measure magnetic gradients in space. In their paper, some cryogenically cooled SQUID-based magnetic gradiometer designs have been considered. SQUID-based magnetic gradiometers are currently under development mainly for airborne geophysical reconnaissance purposes [4][5]. On their own, SQUID gradiometers provide a very high sensitivity to magnetic gradients in the laboratory environment[6], and require some additional auxiliary equipment and a compensation technique when deployed from a moving platform[4]. Due to logistical difficulties, the use of SQUIDS in space has been limited until recently[2][7].

Many fluxgate magnetometers have been previously used in space with sensitivities ranging from $10^{-12}T/\sqrt{\text{Hz}}$ to $10^{-11}T/\sqrt{\text{Hz}}$ [8]. They do not require any cryogenic environment, and fall into a medium range on the sensitivity scale compared to the SQUID-based magnetometers. In the past few years, fluxgate gradiometers have been proposed for space missions. The best performance reported to date is $9.3 \times 10^{-11} \text{ T/m}$ in the band 0.01 Hz to 10 Hz[9].

2 String Magnetic Gradiometer

Recently, a novel Direct String Magnetic Gradiometer (DSMG) has been developed[10][11][12]. It consists of a single aluminium 6061 alloy string or wire (i.e. an object with transverse dimensions much smaller than its longitudinal dimension). The string is held under tension with its second harmonic oscillation mode at $f_0 \approx 850 \text{ Hz}$. An AC current tuned to the second harmonic is used to drive the string. This sets the string into a resonant motion due to the Ampere force per unit length:

$$\frac{\partial \mathbf{f}}{\partial z} = i_s [\mathbf{e}_z \times \mathbf{B}] \sin(\omega t) \quad (1)$$

where \mathbf{e}_z is a unit vector along the Z direction chosen to point along the string's length, i_s is the amplitude of the AC drive current, ω is the string's drive angular frequency and \mathbf{B} is the magnetic induction vector.

When the string is a stretched thin flat ribbon[12], the resonant motion is strictly one-dimensional with its sensitivity axis pointing perpendicular to the plane of motion. In this case, the ribbon represents a one-dimensional mechanical harmonic oscillator having an infinite number of resonant modes[10]:

$$\frac{d}{dt^2}X_n \frac{2}{\tau} \frac{d}{dt}X_n + \omega_n^2 X_n = \left[\frac{2}{\pi n} (1 - (-1)^n) B_y - (-1)^n \frac{2l}{\pi n} \frac{dB_y}{dz} \right] \frac{i_s}{\eta} \sin(\omega t) + N_n(t) \quad (2)$$

It is assumed that the ribbon vibrates in the XOZ plane of its local reference frame the origin of which is coincident with a lower clamp point. The upper clamp point determines the ribbon's length l . $X_n(t)$ is the amplitude of a n -mode mechanical displacement of the ribbon from its unperturbed position aligned with Z axis. It is also assumed that all non-linear terms can be ignored as, in fact, the maximum possible mechanical displacements do not exceed the nanometer scale[13]. In Eq. 2, η is the ribbon's mass per unit length, and τ is its mechanical relaxation time, which is the same for all resonant modes of the ribbon. $N_n(t)$ represents the fundamental thermal noise source (in terms of acceleration noise) which sets an absolute limit on the sensitivity of DSMGs. It has the following correlation function in the white noise area[10]:

$$\langle N_n(t_1) N_m(t_2) \rangle = \frac{8kT}{\eta l \tau} \delta_{nm} \delta(t_1 - t_2) \quad (3)$$

where $k = 1.4 \times 10^{-23}$ J/K is Boltzmann's constant and T is absolute temperature.

As it follows from Eq. 2, the magnetic gradient term of the driving force is coupled only to even resonant modes, while the conventional magnetic field term is coupled to the odd ones.

During operation the string oscillator is an integral part of a dynamic feedback loop[14]. The dynamic properties of such a complex system are different from those of a stand-alone mechanical oscillator described in previous work[10]. In particular, there are a number of additional parameters that can play a crucial role in creating an optimised DSMG with a possibility to implement effective noise suppressing algorithms, such as electronic cooling[15] and pulse feedback modulation technique[16].

By its very nature, DSMG is a modulation-demodulation device. Like flux-gate magnetic gradiometers, it is capable of detecting the quasi DC magnetic gradients both in relative and in absolute units. The detection method provides strong immunity to the uniform magnetic field. Firstly the AC drive current does not couple strongly to the uniform field. The second harmonic drive frequency naturally couples to the magnetic gradient but is well off the drive frequency that couples to the uniform magnetic field. Secondly, the mechanical displacement detection is designed to preferentially detect the second

harmonic oscillations and suppress the fundamental mode oscillations. A common mode rejection ratio of the order of 10^7 is naturally achieved without any balancing technique. The mechanical Q factor of the ribbon provides first stage amplification of the signal to the level where an instrumental read-out noise is lower than the fundamental thermal noise of the ribbon. The latter determines the fundamental rms noise floor of a DSMG[14]:

$$\frac{dB_y}{dz} = \frac{2\pi}{i_s} \sqrt{\frac{2\eta kT^*}{l^3 \tau t}} \quad (4)$$

where, for the current DSMG design, $l = 0.25$ m is the length of the ribbon, $\eta = 8 \times 10^{-6}$ kg/m is the mass per unit length, $\tau \approx 0.1$ s is the relaxation time at a pressure of 1 kPa, $t = 5$ s is the measurement time and T^* is the effective noise temperature. A complete theory of operation of DSMGs is presented in another paper[14].

A DSMG designed to date, operates typically at $T = 300$ K in a 1 kPa vacuum. An inductive read-out system has been developed in order to detect the gradient driven displacements of the ribbon at a level of 6×10^{-13} m/ $\sqrt{\text{Hz}}$. The achieved sensitivity is 1.8×10^{-10} T/m in an unshielded environment in the band 0.0001 Hz to 0.1 Hz.

Below we consider some possible ways of greatly reducing the DSMG's thermal noise limiting factor by using some advantages of the natural space-borne environment. We show that a DSMG specifically designed for space-borne applications can be as sensitive as SQUID-based devices without the requirement of using cryogenic equipment. Also, by their nature, DSMGs should exhibit a very low $1/f$ noise, allowing measurements within the 0.0002 Hz to 0.17 Hz band specified by Hastings et al[3].

3 Thermal noise and the mechanical quality factor

During deployment in space, the DSMG would operate at pressures between 10^{-4} Pa at an altitude of 230 km[17] and 10^{-8} Pa on the moon[18]. This means that despite the large surface area to mass ratio of the ribbon, gas friction damping is negligible. Measurements of the intrinsic mechanical Q factor of Aluminium 6061-T6511 by Duffy[19] with a cylinder of diameter 6mm give Q factors as high as 2.8×10^5 at 300 K. Increasing the Q factor of the ribbon is one way to reduce thermal noise.

The aluminium ribbon is strained and clamped at both ends. Initially the amount of stress in tension is proportional to the amount of strain. The tension

sets the resonant frequency of the magnetic gradiometer. Low levels of stress relaxation are desirable to ensure a long operating life for the DSMG. Table 1 shows that annealed aluminium is not a viable material for the ribbon due to excessive levels of stress relaxation.

For space deployment it is proposed to use a wide thin ribbon. This would maximise the surface area available for thermal radiation which would allow a higher current to be pumped along the ribbon and yet minimise the mass per unit length. The high current and low mass would increase the sensitivity as per Eq. 4.

The mechanical Q factor of a very thin ribbon is lower than the Q factor of the bulk metal because of surface losses. Gretarsson et al give an expression relating Q_{ribbon} to Q_{bulk} [20]:

$$\frac{1}{Q_{ribbon}} = \frac{1}{Q_{bulk}} \left(1 + \mu \frac{d_s}{V/S} \right) \quad (5)$$

where V/S is the volume to surface ratio, d_s is the dissipation depth of surface loss and μ is a measure of the fraction of elastic energy attributable to strains at the surface of the sample. Preliminary experiments by the authors on aluminum 6061 with a ribbon of width 0.125 mm and thickness 0.025 mm in a vacuum of 10^{-2} Pa have measured a ribbon Q factor of 200 ± 20 . In such a thin ribbon the surface loss is dominant. Fitting $Q_{ribbon} = 200$ to Eq. 5 gives:

$$\frac{1}{Q_{ribbon}} = \frac{1}{Q_{bulk}} \frac{2\mu d_s}{t} \quad (6)$$

where $Q_{bulk} = 280000$ is Duffy's result[19], $\mu = 1$, $d_s = 16$ mm and $t = 0.025$ mm is the thickness of the ribbon.

When tension is applied to the ribbon, a portion of the vibration energy is stored as tensile stress instead of surface strains. This can lead to a higher Q factor, also known as an enhanced Q factor. Using a formula in Gonzalez et al[21], the value of μ for the second violin mode is:

$$\mu = \frac{2}{l} \sqrt{\frac{IE}{T}} \quad (7)$$

where l is the length of the ribbon, $I = \frac{t^3 w}{12}$ is the moment of area, w is the width of the ribbon, E is the young's modulus of the aluminum alloy and T is the tension. Substituting in the angular resonant frequency of the second violin mode $\omega = \frac{n\pi}{l} \sqrt{\frac{T}{\rho t w}}$ into Eq. 7 gives:

$$\mu = \frac{4n\pi t}{\omega l^2} \sqrt{\frac{3E}{\rho}} \quad (8)$$

where $\rho = 2690 \text{ kgm}^{-3}$ is the density of aluminum 6061 and $n = 2$ is the mode number. The ribbon Q factor is then:

$$\frac{1}{Q_{ribbon}} = \frac{1}{Q_{bulk}} \frac{8n\pi d_s}{\omega l^2} \sqrt{\frac{3E}{\rho}} \quad (9)$$

In another preliminary experiment, tension was applied to the previously mentioned ribbon of dimensions 0.025 mm by 0.125 mm by 0.25 m. The tension was such that the resonant frequency of the second violin mode was $\omega = 76 \text{ Hz}$. The result was $Q_{ribbon} = 18000$, a proof in principal that the mechanical Q factor of a very thin aluminum ribbon can be enhanced by applying tension.

The proposed ribbon dimensions for the space DSMG are 0.025 mm by 20 mm by 1 m. The proposed ribbon thickness of 0.025 mm is a compromise between the difficulty of machining a thin ribbon and the difficulty of supplying enough current to saturate a thick ribbon. The width of 20 mm and length of 1 m are the maximum dimensions that are feasible for a magnetic gradiometer deployed in space. The DSMG system also requires supporting mechanical structure and electronics so the dimensions of the entire gradiometer are approximately $0.04 \text{ m} \times 0.04 \text{ m} \times 1.1 \text{ m}$.

The sensitivity of the DSMG does not directly depend on the Q factor but on the relaxation time $\tau = \frac{2Q}{\omega}$ of the ribbon. Using Eq. 9, the relaxation time is:

$$\tau = Q_{bulk} \frac{l^2}{4n\pi d_s} \sqrt{\frac{\rho}{3E}} \quad (10)$$

Eq. 10 shows that τ is independent of ω . Nevertheless it is proposed to lower the resonant frequency of the ribbon from 850 Hz to 80 Hz in order to keep the required Q factor to a manageable level. Extrapolating the results of the preliminary experiment, the increased length of 1 m should allow a ribbon Q factor of the order $Q_{ribbon} \approx 300000$ (Q varies as the length of the ribbon squared). The relaxation time would then be approximately $\tau \approx 1200 \text{ s}$ which is much greater than its current value of 0.1 s. The large increase in the relaxation time of the ribbon should produce a significant decrease in the thermal noise as per Eq. 4.

4 Vibration noise

The existing magnetic gradiometer is designed for airborne deployment. The high frequency of 850 Hz allows a mechanical isolator to dampen vibration noise from the aircraft by 120dB. In contrast, the proposed DSMG for space deployment would operate at 80 Hz, a frequency which would short circuit the isolator.

The acceleration noise from solar irradiance fluctuations in near Earth space is on the order of 10^{-10} m/s²/√Hz at 1 mHz[22] and less than 10^{-12} m/s²/√Hz at 80 Hz[23]. This compares with seismic noise of 3×10^{-6} m/s²/√Hz on the ground[24] and engine noise of 3×10^{-2} m/s²/√Hz on a survey aircraft[11].

The reduction of vibration noise by 9 orders of magnitude more than compensates for the greater vibration at lower frequencies. No vibration isolation is required for the proposed DSMG.

5 Operation in the natural space environment

The high current pumped through the ribbon used to detect gradients generates a significant amount of heat. In a high vacuum the dominant method of dissipating this heat is thermal radiation. Table 1 shows that if the ribbon is allowed to heat up to 423 K then the amount of stress relaxation becomes unacceptable. It is therefore proposed that the ribbon not be allowed to heat up past 373 K. For ribbon dimensions as discussed above this limits the maximum current to 4 A (current density of 8×10^6 Am⁻²). From Eq. 4 it is easy to show that the design sensitivity in space is 8×10^{-14} T/m/√Hz.

The entire ribbon would heat up to 373 K and dissipate approximately 0.8 W of power irrespective of the ambient temperature surrounding the ribbon. The T^4 power dependence of thermal radiation means that the DSMG sensitivity depends strongly on the ribbon temperature yet weakly on the environment temperature. Fig. 1 shows that there is little change in sensitivity for environment temperatures ranging from 80 K to 300 K.

6 Thermal radiation in space

In near Earth space while shielded from the Sun, scientific instruments radiating their heat into space can reach cryogenic temperatures between 30 K and 50 K[25]. The advanced sun shields that have been manufactured for the

James Webb Space Telescope can reduce 1370 Wm^{-2} of sunlight impacting on the front of the shield down to a mere $105\mu\text{Wm}^{-2}$ behind the shield where the ambient temperature is approximately 7 K [25][26]. A proposed ribbon made from low resistivity aluminium alloys (described in the next section) would dissipate a tiny 30 mW of power despite a high current of 10 A . High current audio amplifiers are available commercially with output impedances as low as 0.005Ω . Heat dissipated from power supplies and support electronics could be screened from the ribbon by highly reflective mirrors or by displacing all heat producing DSMG modules a meter from the ribbon.

These figures show that passive cooling of the DSMG system in space is feasible. A radiator area of 0.2 m^2 would cool the ribbon down to 40 K , whilst a radiator area of 1 m^2 would cool the system down to 27 K .

7 25 Kelvin to 70 Kelvin operation

At 40 K the electrical resistivity of high purity 99.999% 5N aluminium is very low $\rho \approx 1.80 \times 10^{-10} \Omega\text{m}$ and the thermal conductivity very high $\kappa \approx 2000 \text{ W/m/K}$. The thermal conductivity values are from an empirical fit by Woodcraft[27] and the temperature dependence of resistivity are from Hashimoto et al[28]. These properties make thermal conduction along the axis of the ribbon the dominant form of heat dissipation below 70 K . Fig. 2 shows the temperature profile along the ribbon for an ambient temperature of 40 K .

At temperatures below 10% of the melting point of aluminium, work hardening reduces creep to zero[29] so annealed alloys with low resistivity can be used. Switching the ribbon material from Aluminium 6061 to pure aluminium may be unfeasible since the yield strength of 5N aluminium is only 5 MPa [30]. Instead it is proposed to use special highly conductive high strength alloys such as those developed for the Atlas Project[31][32] as shown in table 2. One alloy of 5N aluminium with 0.1% nickel has a greatly increased yield strength of 80 MPa at a cost of only moderately higher electrical resistivity ($\rho \approx 2.2 \times 10^{-10} \Omega\text{m}$ at 40 K).

The high thermal and electrical conductivities mean that the current could be increased to 10 A and the ribbon width reduced to 18 mm . The current density could be as high as $2 \times 10^7 \text{ Am}^{-2}$. Eq. 4 shows that high currents, low ribbon mass and low temperature increase the signal to noise ratio. The design sensitivity is approximately $10^{-14} \text{ T/m}/\sqrt{\text{Hz}}$ at 40 K .

8 4 Kelvin to 25 Kelvin operation

Further increases in sensitivity are possible if the temperature could be lowered below 25 K by utilizing very large thermal radiators in conjunction with sun shields or by using liquid helium. As shown in table 2, first 5N, then 6N[30] and eventually 7N single-crystal aluminium[33] are necessary to exploit these low temperatures.

For pure metal films, the resistance drops with decreasing temperatures until the mean free path l of conducting electrons becomes larger than the film thickness t . In the limit $l \gg t$ the ribbon resistance will increase by a factor of[34]:

$$\frac{R_{ribbon}}{R_{bulk}} = \frac{4l}{3t \log(l/t)} \quad (11)$$

Using the empirical relationship $l\rho = 8.2 \times 10^{-16} \Omega\text{m}^2$ [35], the mean free path of 7N aluminium with a resistivity of $\rho = 1.5 \times 10^{-13} \Omega\text{m}$ is $l = 5.4 \text{ mm}$. Magnetoresistance reduces the mean free path to 4.7 mm[36]. This value of the mean free path is 187 times larger than the thickness of the ribbon. The resistance of the ribbon would then increase by a factor of 47 due to this size effect. Size effects continue to be significant for temperatures up to 25 K.

The low electrical resistivity at liquid helium temperatures can not be fully realised due to size effects. Other difficulties with exploiting a low temperature environment include magnetoresistance, self inductance and the low strength of pure alloys. Fig. 1 shows that the magnetic gradient sensitivity tapers off below 10K. The design sensitivity at 4 K is approximately $2 \times 10^{-15} \text{ T/m}/\sqrt{\text{Hz}}$ using a current of 10 A and a current density of $2 \times 10^8 \text{ Am}^{-2}$. The small improvement in sensitivity does not justify the difficulty of achieving liquid helium temperatures. DSMGs are only feasible for temperatures between 25 K and 300 K.

9 Low frequency noise background

”The phenomenon of $1/f$ noise, with spectral density scaling inversely with frequency is common to virtually all devices”[37]. The typical frequencies of interest in for global magnetic surveys range from 200 μHz to 0.17 Hz[3]. Deep space missions such as the voyager measure the slowly varying interplanetary magnetic field with frequencies ranging from 50 nHz up to 1 Hz[38]. $1/f$ flicker noise and random walk noise are expected to be significant at these frequencies.

The low frequency noise of the DSMG is compared with some existing devices in this section.

Fluxgate magnetometers have been used in space for more than 30 years. The noise power spectral density of a high performance fluxgate magnetometer is typical of shot noise devices and characterised by a $1/f$ spectrum with a typical value of $3 \times 10^{-12} T/\sqrt{\text{Hz}}$ at 1 Hz for space research-grade instruments[8]. The source of the noise is attributed to Barkhausen-like mechanisms that affect the motion of domains in ferromagnetic material in the sensor cores[2]. One fluxgate magnetic gradiometer built for use in space has a sensitivity of $3 \times 10^{-11} \text{ T/m}/\sqrt{\text{Hz}}$ at 1 Hz[9].

Low T_c SQUIDs were proposed as a highly sensitive magnetic gradiometer for space-borne magnetic investigations more than 20 years ago[3]. SQUIDs have the best sensitivity on offer for terrestrial operations. One low T_c SQUID gradiometer has a sensitivity of $6 \times 10^{-14} \text{ T/m}/\sqrt{\text{Hz}}$ [4] in the laboratory with a $1/f$ noise corner at 0.3 Hz. $1/f$ flicker noise is more severe in high T_c gradiometers which have a typical $1/f$ noise corner of 10Hz[39][5]. The two major sources of $1/f$ noise in dc SQUIDs are fluctuations of the critical current in the Josephson junctions and motion of flux lines (vortices) trapped in the body of the SQUID[6]. The frequency ranges of interest in space exploration are entirely within the $1/f$ noise region of SQUIDs[3].

Previously, all existing gradiometers measured the gradient from the differential output of two sensing elements. Uniform fields contaminate the results since the common mode rejection ratio of gradiometers is finite. Typically the common mode rejection ratio is on the order of 10^4 [4][39][40] although rotating gradiometers can do better[5]. The common mode rejection ratio tends to decrease with time[40] which introduces additional noise at very low frequencies.

The noise performance of magnetometers is strongly affected by mechanical and thermal stresses, which vary over time and with exposure to extreme environments. Even state of the art magnetometers experience drift on the order of 10^{-10} T/year [2]. These mechanical and thermal effects introduce a random walk noise with power scaling $1/f^2$.

Because the DSMG is a single element device, any drifts associated with non-stationary unbalance of two different sensors (as in the case of multisensor based gradiometers) are absent. Also, it is a modulation-demodulation device such that most of the $1/f$ noise in the DC region is suppressed compared to static gradiometers.

The low frequency noise of the DSMG is characterised by a $1/f^2$ spectrum of random walk noise. In the closed loop operation[14], the ground based DSMG has a $1/f^2$ noise corner of approximately 2.5 mHz (see Fig. 3). With

the feedback loop turned off, the frequency of the noise corner depends on the magnitude of the external gradient; noise corners as high as 0.2 Hz have been measured when the DSMG is exposed to gradients higher than 10000 nT/m.

10 Low frequency noise improvements

The white noise floor of the space DSMG is lower than the ground based DSMG by several orders of magnitude. If the level of random walk noise remains the same then the frequency of the $1/f^2$ noise corner would increase. The origins of the low frequency noise in the DSMG are not known at present although several models have been proposed. However, there are reasons for believing that the level of low frequency noise can be reduced step in step with the white noise.

Any mismatch between the drive frequency of the AC current and the resonant ribbon frequency creates low frequency noise. The space DSMG's low level of white noise would allow more accurate tracking of the ribbon resonant frequency. In addition, the amplitude of ribbon vibrations during closed loop operation could be reduced step in step with the white noise. By using the feedback of closed loop operation to reduce the signal[14], any amplitude dependant low frequency noise will be reduced accordingly.

The very high mechanical Q factor of the space DSMG could be utilised for off resonance operation. The very large signal at resonance could be used exclusively to identify the exact resonant frequency of the ribbon. The level of signal at resonance could be ignored. The difference between the AC current drive frequency and the resonant frequency would be known exactly. Amplitude fluctuations from frequency drift could be fully compensated while any small variance in the mechanical Q would produce only negligible noise during off resonance operation.

For the reasons outlined above, the noise spectrum of the proposed DSMG for space applications is expected to be flat for frequencies down to 2.5 mHz. Fig. 3 compares the expected performance of the DSMG with other technologies and shows predominance of $1/f$ noise and $1/f^2$ noise at low frequencies.

11 Readout

In addition to the thermal noise in the ribbon, there is also measurement noise in the apparatus used to measure the position of the ribbon. In the

limit $Q \rightarrow \infty$, the rms displacement x of the ribbon produced by a magnetic gradient is:

$$x = \frac{dB_y}{dz} \frac{li}{n\pi^3\sqrt{32}\eta f_0 f} \quad (12)$$

where $n = 2$ is the mode number, l is the length of the ribbon, η is the mass per unit length, i is the peak current, f_0 is the resonant frequency of the 2nd violin mode of the ribbon and f is the frequency of the magnetic gradient signal. For ground based operations, the smallest detectable signal of 4×10^{-10} T/m/ $\sqrt{\text{Hz}}$ produces a displacement of 10^{-11} m/ $\sqrt{\text{Hz}}$ over a bandwidth of 1 Hz.

The present method of measuring ribbon deflections is pumping the ribbon with a small radio frequency current of $i = 0.2$ A. The radio frequency current generates a radio frequency flux around the ribbon. Two pickup coils connected in differential mode measure the modulation in flux as the ribbon moves. Each pickup coil is capable of measuring ribbon deflections of size 6×10^{-13} m/ $\sqrt{\text{Hz}}$ which is sufficient to detect the minimum signal.

If the sensitivity improvements suggested in this paper are implemented then the minimum signal amplitude will be only 9×10^{-15} m/ $\sqrt{\text{Hz}}$ for a 1 Hz signal. In order to improve the readout sensitivity enough to detect a displacement this small, the pickup coils could be replaced with a microwave cavity readout developed for gravitational wave antennas[41]. Other solutions include a low noise SQUID[42] or optical readout using a Fabry Perot cavity[43].

12 Conclusion

The proposed space DSMG has a sensitivity of 8×10^{-14} T/m/ $\sqrt{\text{Hz}}$ using only the natural space environment. Even higher sensitivity is possible with passive cooling of the DSMG in space. The size of the DSMG and the power consumption requirements are comparable with existing magnetometers used in space missions. It is also possible to deploy a full tensor gradiometer by combining several single axis DSMGs.

Acknowledgements

The authors would like to thank Mr. Howard Golden of Gravitec Instruments for many useful discussions and suggestions. Work on the DSMG project is funded in part by a linkage grant from the Australian Research Council.

References

- [1] E.I. Alves, V.M.C. Madeira, Rationale for the deployment of a magnetic gradiometer on Mars, Proceedings of the Sixth International Conference on Mars (2003) paper 3014.
- [2] M.H. Acuna, Space-based magnetometers, Review of Scientific Instruments 73 (2002) 3717-3736.
- [3] R. Hastings, R.P.S. Mahler, R.S. Schneider Jr., J.H. Eraker, Cryogenic magnetic gradiometers for space applications, IEEE Transactions on Geoscience and Remote Sensing GE-23 (1985) 552-561.
- [4] R. Stolz, V. Zakosarenko, M. Schulz, A. Chwala, L. Fritsch, H.G. Meyer, E.O. Kostlin, Magnetic full-tensor SQUID gradiometer system for geophysical applications, The Leading Edge 25 (2006) 178-180.
- [5] D. Tilbrook et al, Design and development of a SQUID tensor gradiometer, in: Applied Superconductivity Conference, Houston, 2002.
- [6] R.L. Fagaly, Superconducting quantum interference device instruments and applications, Review of Scientific Instruments 77 (2006) 101101.
- [7] M. Klinger, J.H. Hinken, S.S. Tinchev, First space test of high-Tc SQUIDs, IEEE Transactions on Applied Superconductivity 5 (1995) 2759-2761.
- [8] F. Primdahl, J.R. Petersen, G. Marklund, N. Olsen, P. Brauer, T. Risbo, A. Ranta, MAIDS: Magnetic investigation in deep space, Science instrument proposal to ESA for the SMART-1 mission, Danish Space Research Institute - Technical University of Denmark, 1998.
- [9] J.M.G. Merayo, P. Brauer, F. Primdahl, Triaxial fluxgate gradiometer of high stability and linearity, Sensors and Actuators A 120 (2005) 71-77.
- [10] A.V. Veryaskin, Magnetic gradiometry: a new method for magnetic gradient measurements, Sensors and Actuators A 91 (2001) 233-235.
- [11] W. McRae, A.V. Veryaskin, L. Ju, D.G. Blair, E. Chin, J. Dumas, B. Lee, String magnetic gradiometer system: recent airborne trials, SEG Expanded Abstracts 23 (2004) 790-793.
- [12] H. Golden, W. McRae, A. Sunderland, A.V. Veryaskin, D.G. Blair, L. Ju, A novel magnetic gradiometer: description, design issues, and trial results, in: Australian Institute of Physics 17th National Congress, Brisbane, 2006.
- [13] G.V. Anand, Nonlinear resonance in stretched strings with viscous damping, The Journal of the Acoustical Society of America 50 (1966) 1517-1528.
- [14] A.V. Veryaskin, Theory of operation of direct string magnetic gradiometer with proportional and integral feedback, `arXiv:0712.0908[physics,inst-det.]`, 2007.

- [15] R.C. Ritter, G.T. Gillies, Classical limit of mechanical thermal noise reduction by feedback, *Physical Review A* 31 (1985) 995-1000.
- [16] A.V. Veryaskin (to be presented at INTERMAG2008, Madrid, Spain).
- [17] National Aeronautics and Space Administration, Earth Atmospheric Model, <http://www.grc.nasa.gov/WWW/K-12/airplane/atmosmet.html>
- [18] G.A. Landis, Degradation of the lunar vacuum by a moon base, *Acta Astronautica* 21 (1990) 183-187.
- [19] W. Duffy Jr. , Acoustic quality factor of aluminium and selected aluminium alloys from 50 mK to 300 K, *Cryogenics* 42 (2002) 245-251.
- [20] A.M. Gretarsson, G.M. Harry, Dissipation of mechanical energy in fused silica fibers, *Review of Scientific Instruments* 70 (1999) 4081-4087.
- [21] G.I. Gonzalez, P.R. Saulson, Brownian motion of a mass suspended by an anelastic wire, *The Journal of the Acoustical Society of America* 96 (1994) 207-212.
- [22] B.L. Schumaker, Disturbance reduction requirements for LISA, *Classical and Quantum Gravity* 20 (2003) S239-S253.
- [23] J. Pap, M. Anklin, C. Frohlich, C. Wehrli, F. Varadi, L. Floyd, Variations in total solar and spectral irradiance as measured by the VIRGO experiment on SOHO, *Advances in Space Research* 24 (1999) 215-224.
- [24] D. Coward, J. Turner, D.G. Blair, Characterizing seismic noise in the 2-20 Hz band at a gravitational wave observatory, *Review of scientific instruments* 76 (2005) 044501.
- [25] Space Telescope Science Institute, JWST Design: Sunshield, <http://www.stsci.edu/jwst/overview/design/sunshade.html>
- [26] M.J. Amato, D.J. Benford, Harvey S. Moseley, J. Roman, An engineering concept and enabling technologies for a large single aperture far-infrared observatory (SAFIR), *Proceedings of SPIE* 4850 (2003) 1120-1131.
- [27] A. Woodcraft, Predicting the thermal conductivity of aluminium alloys in the cryogenic to room temperature range, *Cryogenics* 45 (2005) 421-432.
- [28] E. Hashimoto, Y. Ueda, Zone refining of high-purity aluminum, *Materials Transactions JIM* 35 (1994) 262-265.
- [29] H.J. Frost, M.F. Ashby, *Deformation mechanisms maps: the plasticity and creep of metals and ceramics*, Pergamon Press, New York, New York USA: Pergamon Press, 1982, ch. 4.
- [30] R.P. Reed, Aluminum 2. a review of deformation properties of high purity aluminium and dilute aluminium alloys, *Cryogenics* 12 (1972) 259-291.
- [31] K. Wada et al, Development of high-strength and high-RRR aluminum-stabilized superconductor for the ATLAS thin solenoid, *IEEE Transactions on applied superconductivity* 10 (2000) 373-376.

- [32] K. Wada, S. Meguro, H. Sakamoto, A. Yamamoto, Y. Makida, High-strength and high-RRR ALNi alloy for aluminum-stabilized superconductor, *IEEE Transactions on applied superconductivity* 10 (2000) 1012-1015.
- [33] E. Hashimoto, Y. Ueda, T. Kino, Purification of ultra-high purity aluminum, *Journal de Physique IV* 5 (1995) 153-157.
- [34] E.H. Sondheimer, The mean free path of electrons in metals, *Advances in Physics* 1 (1952) 1-42.
- [35] J.R Sambles, K.C. Elsom, G. Sharp-Dent, The effect of sample thickness on the resistivity of aluminium, *Journal of Physics F: Metal Physics* 11 (1981) 1075-1092.
- [36] J.P. Egan, R.W. Boom, Measurement of the electrical resistivity and thermal conductivity of high purity aluminium in magnetic fields, *Advances in Cryogenic Engineering (Materials)* 36A (1990) 679-686.
- [37] R.H. Koch, D.P. DiVincenzo, J. Clarke, Model for 1/f flux noise in SQUIDs and qubits, *Physical Review Letters* 98 (2007) 267003.
- [38] L.F. Burlaga, C. Wang, J.D. Richardson, Large-scale magnetic field sluctuations and development of the 1999–2000 global merged interaction region: 1-60 AU, *The Astrophysical Journal* 585 (2003) 1158-1168.
- [39] Y. Zhang et al, A HTS SQUID gradiometer using superconducting coplanar resonators for operation in unshielded environment, *Chinese Journal of Physics* 38 (2000) 330-338.
- [40] M. Bick et al, Highly balanced long-baseline axial gradiometer based on high-Tc superconducting tape, *IEEE Transactions on Applied Superconductivity* 15 (2005) 765-768.
- [41] E.N. Ivanov, M.E. Tobar, P.J. Turner, D.G. Blair, Noncontacting microwave coupling to a cryogenic gravitational wave antenna, *Review of Scientific Instruments* 64 (1993) 1905-1909.
- [42] P. Carelli, M.G. Castellano, G. Torrioli, R. Leoni, Low noise multiwasher superconducting interferometer, *Applied Physics Letters* 72 (1998) 115-117.
- [43] L. Conti, M. De Rosa, F. Marin, L. Taffarello, M. Cerdonio, Room temperature GW bar detector with opto-mechanical readout, *Journal of Applied Physics* 93 (2003) 3589-3595.
- [44] J.G. Kaufman, Tensile, creep and fatigue data at high at high and low temperatures, *The Aluminum Association, Washington DC*, p. 166.
- [45] National Aeronautics and Space Administration, Technology readiness overview mixed signal devices for very low temperatures background, <http://nepp.nasa.gov/index.nasa.cfm/898/>

Temperature	Loss in stress after 14 months	
	Al 6061-O	Al 6061-T6
278 K	27%	5%
373 K	62%	16%
423 K	100%	43%
450 K	100%	62%
478 K	100%	67%

Table 1

The results in this table are taken from Kaufman[44]. Stress relaxation becomes increasingly problematic at higher temperatures. Tempering the aluminium (Al 6061-T6) can reduce stress relaxation compared with fully annealed aluminium (Al 6061-O).

Alloy	Temper	Yield strength	Q at 300K	Q at 10K	RRR
Al 6061	T6511	275MPa	280000	3700000	3
5N Al + 2% Ni	Cold worked	120MPa			170
5N Al + 0.1% Ni	Cold worked	80MPa			590
5N Al + 0.2% Ce	Cold worked	46MPa			1400
5N Al	Annealed	5MPa	45000	220000	6000
6N Al	Annealed	5MPa			45000
7N Al	Single crystal	0.7MPa			> 300000

Table 2

At progressively lower temperatures, aluminium alloys[44][31][30][33] with lower and lower values of electrical resistance are proposed. The low resistance comes at the expense of a reduced yield strength. RRR (residual resistivity ratio) is the ratio of the electrical resistivity at room temperature to the residual resistivity from impurities at liquid helium temperatures.

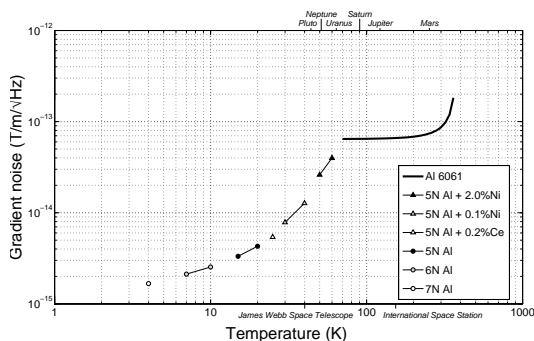


Fig. 1. String Magnetic Gradiometer design sensitivities as a function of ambient temperature. There is very little advantage in cooling the DSMG down to a temperature of 70 K. Further decreases in temperature below 70 K can however, deliver large increases in sensitivity. The ambient temperatures of electronics exposed to sunlight near the outer planets are shown together with the temperature of some satellites in near earth orbits which are shielded from the Sun[45].

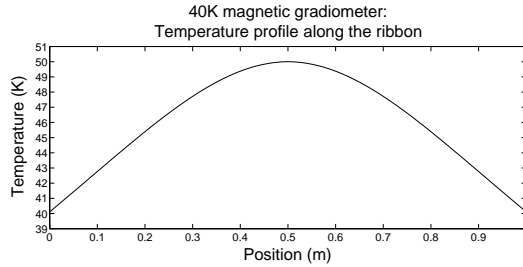


Fig. 2. 0.03 W of power is dissipated by thermal conduction along the 1 m length of the ribbon. The middle of the ribbon heats up to 50 K while the ends are in thermal contact with a heat sink at 40 K.

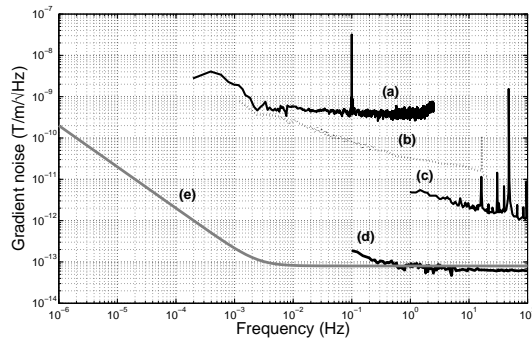


Fig. 3. The magnetic gradient system noise of (a) an existing DSMG operating in a moderate vacuum of 1 kPa in unshielded environment, (b) a fluxgate gradiometer developed for magnetic surveying from a satellite[9], (c) a high temperature SQUID gradiometer developed for magnetocardiography[39], (d) a low temperature SQUID gradiometer developed for airborne mineral exploration[4] and (e) the proposed space DSMG in high vacuum.